Nitric Oxide Binding to Ferric Cytochrome P450: A Computational Study

Damián A. Scherlis,[†] Cora B. Cymeryng,[‡] and Darío A. Estrin*[,†]

Departamento de Química Inorgánica, Analítica y Química-Física and INQUIMAE, Facultad de Ciencias Exactas y Naturales, Universidad de Buenos Aires, Ciudad Universitaria—Pab II, 1428 Buenos Aires, Argentina, and Departamento de Bioquímica Humana, Facultad de Medicina, Universidad de Buenos Aires, Paraguay 2155, Buenos Aires, Argentina

Received October 8, 1999

The interaction between nitric oxide (NO) and the active site of ferric cytochrome P450 was studied by means of density functional theory (DFT), at the generalized gradient approximation level, and of the SAM1 semiempirical method. The electrostatic effects of the protein environment were included in our DFT scheme by using a hybrid quantum classical approach. The active-site model consisted of an iron(III) porphyrin, the adjacent cysteine residue, and one coordinated water molecule. For this system, spin populations and relative energies for selected spin states were computed. Interestingly, the unpaired electron density, the HOMO, and the LUMO were found to be highly localized on the iron and in an appreciable extent on the sulfur coordinated to the metal. This provides central information about the reactivity of nitric oxide with the active site. Since the substitution of a molecule of H_2O by NO has been proposed as being responsible for the inhibition of the cytochrome in the presence of nitric oxide, we have analyzed the thermodynamic feasibility of the ligand exchange process. The structure of the nitrosylated active site was partially optimized using SAM1. A low-spin ground state was obtained for the nitrosyl complex, with a linear Fe−N−O angle. The trends found in Fe−N−O angles and Fe−N lengths of the higher energy spin states provided a notable insight into the electronic configuration of the complex within the framework of the Enemark and Feltham formalism. In relation to the protein environment, it was assessed that the electrostatic field has significant effects on several computed properties. However, in both vacuum and protein environments, the ligand exchange reaction turned out to be exergonic and the relative orders of spin states of the relevant species were the same.

Introduction

Cytochrome P450[1] enzymes take part in the oxidation of a large variety of structurally diverse compounds. These enzymes are referred to as monooxygenases because they catalyze the incorporation of an atom of O_2 into a substrate, while the other atom is reduced to water. Cytochrome P450 monooxygenases are responsible for essential physiological transformations and also play a role in the detoxification of potentially dangerous compounds.[2−5] Among their functions, in fact, is the catalysis of hydroxylation reactions involved in the synthesis of all steroid hormones. Nitric oxide (NO) is a small, gaseous, and reactive molecule associated with the regulation of a wide range of biological functions. Several lines of evidence indicate that NO might affect steroidogenesis, and P450 enzymes have been suggested as the target for NO action.[6,7]

Although the catalytic cycle of the enzyme is well-known, the mechanism through which the nitric oxide modulates P450 activity has not been completely established. All P450 cytochromes contain a heme group attached to the protein via a thiolate linkage between the iron and the sulfur atom of a cysteine (see Figure 1). In the first stage of the cycle in the substrate-free cytochrome, a water molecule is axially coordinated to the iron atom of the heme. After binding the substrate, the water molecule is released and the metal center is reduced from Fe(III) to Fe(II).[2−5] A promotion of the spin state is known to accompany this transformation, in accordance with the correlation between coordination number and spin state observed in iron porphyrins. In fact, most pentacoordinated iron porphyrins are reported to be high spin.[8] The next step in the enzymatic cycle involves the binding of dioxygen and the subsequent return to the low-spin configuration. According to current proposals for the mechanism, this step is followed by the formation of a ferryl oxygen species and then the hydroxylation of substrate.[2−5] In this work, we examine the interaction between the heme iron(III) of the cytochrome and the nitric oxide as a possible means of inactivation of the enzyme. Our purpose is to analyze the thermodynamic feasibility of the displacement of H_2O by NO, which would eventually block the active site. There have been a large number of quantum mechanical calculations performed on model systems of the active site of hemoglobin, P450, and

* Corresponding author. Fax: 54-11-4576-3341. E-mail: dario@q1.fcen.uba.ar.
† Facultad de Ciencias Exactas y Naturales.
‡ Facultad de Medicina.

(1) Hereafter, we will adopt the usual designation of P450 to denote cytochrome P450.
(2) (a) Lewis, D. F.; Pratt, J. M. *Drug Metab. Rev.* **1998**, *30*, 739. (b) Poulos, T. L. *Curr. Opin. Struct. Biol.* **1995**, *5*, 767.
(3) Ortiz de Montellano, P. R. *Cytochrome P-450: Structure, Mechanism and Biochemistry*; Plenum Press: New York, 1995.
(4) Guengerich, F. P.; MacDonald, T. L. *FASEB J.* **1990**, *4*, 2453.
(5) Dawson, J. H.; Sono, M. *Chem. Rev.* **1987**, *87*, 1255.
(6) (a) Hanke, C. J.; Drewett, J. G.; Myers, C. R.; Campbell, W. B. *Endocrinology* **1998**, *139*, 4053. (b) del Punta, K.; Charreau, E. H.; Pignataro, O. *Endocrinology* **1996**, *137*, 5337. (c) Van Voorhis, B. J.; Dunn, M. S.; Snyder, G. D.; Weiner, C. P. *Endocrinology* **1994**, *135*, 1799.
(7) Minamiyama, Y.; Takemura, S.; Imaoka, S.; Funae, Y.; Tanimoto, Y.; Inoue, M. *J. Pharmacol. Exp. Ther.* **1997**, *283*, 1479.
(8) Marques, H. M.; Munro, O. Q.; Grimmer, N. E.; Levendis, D. C.; Marsicano, F.; Pattrick, G.; Markoulides, T. *J. Chem. Soc., Faraday Trans.* **1995**, *91*, 1741.

10.1021/ic991191d CCC: $19.00
Published on Web 05/06/2000

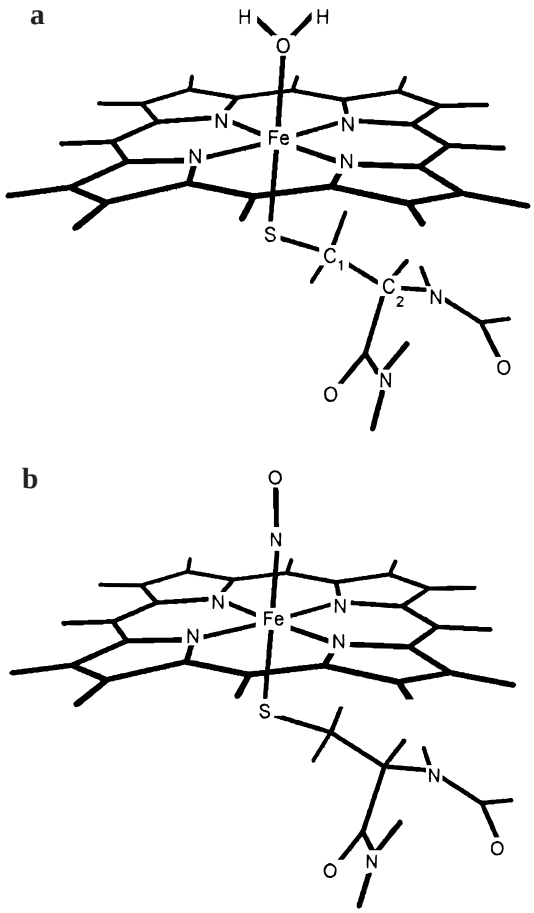

Figure 1. Model of the active site of ferric cytochrome P450 in the ground state: (a) aquo complex; (b) nitrosyl complex.

related systems.[9−17] Many have investigated the coordination of O_2 or CO to the metal, but none have included the nitrosyl or the aquo heme adduct for the particular case of P450. Density functional theory (DFT) methods have been used with success in these kinds of systems,[9−12] and comparison against spectroscopic data (Mossbauer, NMR, X-ray, and EPR, specially) has confirmed that this theory is appropriate for the evaluation of paramagnetic states.[13−15] Unlike other quantum mechanical techniques, such as Hartree−Fock molecular orbital theory, DFT accounts for the correlation energy, which may be needed when high-spin configurations are computed. Recently, by means of DFT, Rovira and Parrinello predicted geometries and spin states of iron porphyrins with three different diatomic ligands: O_2, CO, and NO.[16] To reproduce the local protein environment in hemoglobin, they included an imidazole axial ligand. de Groot and co-workers[17] optimized the high-spin structure of iron(II) and iron(III) *S*-methyl porphyrin models of the five-coordinated complexes in P450. Harris, Loew, and Waskell[14] used DFT at the generalized gradient approximation (GGA) level to calculate two oxidative intermediates of the cytochrome monooxygenation cycle on the basis of the same model compound. A recent work of Green, also based on DFT computations,[12a] analyzes the nature of the iron−sulfur bond and the role of the thiolate axial ligand in connection with the spin state of the resting cytochrome P450.

Table 1. Crystallographic Parameters of Iron Porphyrins with a Cysteine Ligand, Corresponding to Different Heme Proteins (Distances, Å; Angles, deg)[a]

	X-ray structures			
	P450 Bm3[c]	P450 Bm3[d]	P450 Cam[e]	CPO[f]
coordn no.	6	6	5	5
Fe−N[b]	1.99	1.99	2.02	2.04
Fe−S	2.04	2.11	2.34	2.35
Fe−O	1.95	1.89		
Fe−S−C	111.7	107.6	108.8	107.5
S−Fe−O	177.3	176.3		

[a] The metal center is either five- or six-coordinated, depending on experimental conditions. [b] Mean lengths. [c] Reference 18. [d] Reference 47a. [e] Reference 47b. [f] Reference 47c.

In the present study, we employed DFT and a semiempirical technique to find the spin ground states of the aquo and the nitrosyl heme complexes in ferric cytochrome P450, as well as the energetic change corresponding to the ligand exchange. Also, to estimate the extent of the protein effect on the heme moiety electronic structure, we performed the calculations using a hybrid quantum classical approach, adding the electrostatic field derived from a distribution of point charges that represents the rest of the enzyme. The quantum subsystem selected to model the active site consists of the iron porphyrin and the cysteine ligand, with a geometry taken from the X-ray structure of a native P450 cytochrome.[18] We included the whole amino acid in the system to account for the effects of the immediate atoms on the sulfur electronic density, directly implicated in the behavior of the metal complex. The calculations provide information concerning relative energies, the unpaired spin density, and the electronic configuration in terms of one-electron orbitals as well. In several ways, these data contribute to the interpretation and understanding of the inhibition mechanisms of P450, in particular, and, in a broader context, of the chemistry of heme derivatives with nitric oxide.

Methods

Model of the Active Site. The system used to model the active site comprises the iron porphyrin plus the cysteine residue adjacent to the metal, including the amide linkages (Figure 1). The geometry corresponds to the X-ray structure of the cytochrome P450 monooxygenase given in ref 18 and summarized in Table 1. Lateral substituents of the protoporphyrin were neglected, and hydrogens were added to the crystallographic structure using the HyperChem 5.1 Pro interface.[19] The crystal structure corresponds to substrate-free cytochrome, in which a water ligand is coordinated to the heme iron. Taking into account the fact that in the protein the active site is constrained to a geometry that would be different from the relaxed gas phase configuration, we did

(9) (a) Ghosh, A.; Almlof, J.; Lawrence, Q., Jr. *J. Phys. Chem.* **1994**, *98*, 5576. (b) Ghosh, A.; Bocian, D. F. *J. Phys. Chem.* **1996**, *100*, 6363. (c) Matsuzawa, N.; Ata, M.; Dixon, D. A. *J. Phys. Chem.* **1995**, *99*, 7698.
(10) Jones, D. H.; Hinman, A. S.; Ziegler, T. *Inorg. Chem.* **1993**, *32*, 2092.
(11) (a) Havlin, R. H.; Godbout, N.; Salzmann, R.; Wojdelski, M.; Arnold, W.; Schulz, C. E.; Oldfield, E. *J. Am. Chem. Soc.* **1998**, *120*, 3144. (b) Spiro, G. T.; Kozlowski, P. M. *J. Am. Chem. Soc.* **1998**, *120*, 4524.
(12) (a) Green, M. T. *J. Am. Chem. Soc.* **1998**, *120*, 10772. (b) Green, M. T. *J. Am. Chem. Soc.* **1999**, *121*, 7939.
(13) Harris, D.; Loew, G. H.; Komornicki, A. *J. Phys. Chem. A* **1997**, *101*, 3959.
(14) Harris, D.; Loew, G. H.; Waskell, L. *J. Am. Chem. Soc.* **1998**, *120*, 4308.
(15) Henson, N. J.; Hay, P. J.; Redondo, A. *Inorg. Chem.* **1999**, *38*, 1618.
(16) (a) Rovira, C.; Kunc, K.; Hutter, J.; Ballone, P.; Parrinello, M. *J. Phys. Chem. A* **1997**, *101*, 8914. (b) Rovira, C.; Parrinello, M. *Int. J. Quantum Chem.* **1998**, *70*, 387. (c) Rovira, C.; Ballone. P.; Parrinello, M. *Chem. Phys. Lett.* **1997**, *271*, 246.
(17) de Groot, M. J.; Havenith, R. W. A.; Vinkers, H. M.; Zwaans, R.; Vermeulen, N. P. E.; van Lenthe, J. H. *J. Comput.-Aided Mol. Des.* **1998**, *12*, 183.
(18) Yeom, H.; Sligar, S. G.; Li, H.; Poulos, T. L.; Fulco, A. J. *Biochemistry* **1995**, *34*, 14733.
(19) *HyperChem*, Release 5.1 Pro; Hypercube, Inc.: Gainesville, FL, 1997.

Table 2. Selected Geometrical Parameters of the $[Fe(CN)_6]^{4-}$ and $[Fe(CN)_5NO]^{2-}$ Anions (Distances, Å; Angles, deg)[a]

	$[Fe(CN)_6]^{4-}$			
	SAM1	DFT-GGA[b]	DFT-LDA	exptl[c]
Fe−C	2.000	1.976	1.886	1.93
C−N	1.172	1.197	1.192	1.17
	$[Fe(CN)_5NO]^{2-}$			
	SAM1	DFT-GGA[d]	DFT-LDA	exptl[e]
$Fe-C_{eq}$[f]	1.967−1.971	1.948−1.960	1.896−1.900	1.928−1.936
Fe−NO	1.592	1.652	1.621	1.652
$(C-N)_{ax}$	1.156	1.180	1.175	1.150
$(C-N)_{eq}$	1.153	1.181	1.173	1.153
$C_{eq}-Fe-C_{eq}$	170.7	168.8	167.7	169.1

[a] SAM1 and LDA data were obtained in this work. [b] Reference 22a. [c] Reference 23. [d] Reference 22b. [e] Reference 24. [f] Two values are shown since the four equatorial Fe−C bonds are not equivalent.

not perform any geometry optimization on the aquo complex. Because packing interactions between macromolecules in a crystal are so few and because they are often indirect, through one or several layers of solvent molecules, these interactions seldom change the overall structure of the protein, except for a few side chains.[20] Consequently, we consider the X-ray coordinates to represent more accurately the active enzyme than the vacuum optimized structure. In the case of the nitrosyl P450 complex, for which there is no X-ray structure available, we assumed the same geometry of the active site, but the position of the NO molecule was optimized through SAM1 (semi ab initio method, version 1) calculations.[21]

SAM1 Calculations. The SAM1 computations were done at the unrestricted Hartree−Fock (UHF) level in all cases. To validate the semiempirical method, it was tested on different isolated cyanoiron complexes and iron porphyrins. Selected geometrical parameters predicted by SAM1 and DFT computations at the LDA and GGA levels[22] and experimental results[23,24] are shown in Table 2 for the $[Fe(CN)_6]^{4-}$ and $[Fe(CN)_5NO]^{2-}$ ions. It has been established that, for these types of compounds, DFT calculations performed at the local density approximation (LDA) level tend to yield slightly shorter metal−ligand distances and better agreement with experiments than DFT calculations at the GGA level.[25] The overall quality of the SAM1 optimized geometries in these systems is similar to that obtained using DFT-GGA calculations.

The semiempirical method was also tested on ferrous porphyrins with diatomic ligands. Table 3 shows the geometrical parameters obtained with SAM1. In the same table are included the results corresponding to recent DFT-GGA optimizations,[16a] together with experimental values from model systems. The SAM1 optimized geometries turned out to be as good as or even superior to what could be expected for higher level calculations, with errors smaller than 4% in distances and angles relative to experimental structures. An exception is the X−O length (see Table 3), which SAM1 systematically overestimates; this is also observed in the case of DFT, especially for the nitrosyl ligand. Regarding this aspect, it has been suggested that the N−O distance of the crystal structure is largely underestimated.[16a] To assess the reliability of the calculations on the higher energy spin states, the isolated Fe(II) porphyrin was partially optimized at three different spin multiplicities. The ground spin state was a triplet, in agreement to what has been stated experimentally for related compounds, such as iron(II) tetraphenylporphyrin.[26] The adiabatic excitation energies to the singlet and quintet states were calculated to be 11.9 and 14.6 kcal/mol, respectively, while DFT computations[16] provided energy differences of 12.7 and 14.7 kcal/mol.

Table 3. Structural Parameters of Iron(II) Porphyrin Complexes with Diatomic Ligands XO Optimized with SAM1 (X = C, N, O) (Bond Lengths, Å; Angles, deg)[a]

		FePCO	FePNO	$FePO_2$
Fe-X	SAM1	1.72	1.65	1.76
	DFT	1.69	1.69	1.74
	exptl	1.77	1.71	1.75
X−O	SAM1	1.20	1.18	1.26
	DFT	1.17	1.19	1.28
	exptl	1.12	1.12	1.15−1.17[b]
Fe-X−O	SAM1	180	153	115
	DFT	180	150	123
	exptl	179	149	120[c]
$Fe-N_p$	SAM1	2.03	2.00	2.01
	DFT	1.99	2.02	2.00
	exptl	2.02	2.00	1.98
refs	SAM1	this work	this work	this work
	DFT	16a	16a	16a
	exptl	48a	48b	48c

[a] In the cases of the CO and O_2 species, the trans ligand is imidazole. The FePNO complex is five-coordinate. $Fe-N_p$ indicates the averaged distance to the nitrogens of the porphyrin ring. [b] The O−O separation is unrealistically short when compared to the molecular oxygen O−O distance of 1.21 Å. An off-axis displacement of the bonded oxygen atom seems to be probable.[48c] [c] The Fe−O−O angle varies from one crystal structure to the other. In fact, the SAM1 potential energy surface is quite flat between 110 and 125. 120° is the mean value in oxymyoglobin.[49]

Density Functional Calculations. A Gaussian basis set implementation of DFT (Molecole-DFT package)[27] was used to compute single-point energies of the aquo and nitrosyl active site. The Kohn−Sham self-consistent procedure[28] was applied for obtaining the electronic density and energy through the expansion of a set of one-electron orbitals. Matrix elements of the exchange-correlation potential were calculated by a numerical integration scheme.[29] Double-ζ valence polarization (DZVP) basis sets developed for DFT calculations by Godbout et al.[30] were used for C, N, O, H, and S atoms. For iron, the DZV basis set given in ref 31 was chosen. The contraction patterns were (4333/431/41) for Fe, (6321/521/1) for S, (41) for H, and

(20) Branden, C.; Tooze, J. *Introduction to Protein Structure*; Garland Publishing, Inc.: New York and London, 1991.
(21) (a) *AMPAC 5.0*, 1994 Semichem: Shawnee, KS, 1994. (b) Holder, A. J.; Ward, R. *Abstr. Pap.—Am. Chem. Soc.* **1998**, *216*, 174. (c) White, D. A.; Holder, A. J.; Jie, C. *Abstr. Pap.—Am. Chem. Soc.* **1998**, *216*, 182.
(22) (a) Estrin, D.; Hamra, O. Y.; Paglieri, L.; Slep, L.; Olabe, J. *Inorg. Chem.* **1996**, *35*, 6832. (b) Estrin, D.; Baraldo, L.; Slep, L.; Barja, B.; Olabe, J.; Paglieri, L.; Corongiu, G. *Inorg. Chem.* **1996**, *35*, 3897.
(23) Taylor, J. C.; Mueller, M. H.; Hitterman, R. L. *Acta Crystallogr.* **1974**, *A26*, 559.
(24) Bottomley, F.; White, P. S. *Acta Crystallogr.* **1979**, *B35*, 2193.
(25) Bray, M.; Deeth, R.; Paget, V.; Sheen, P. *Int. J. Quantum Chem.* **1996**, *61*, 85.
(26) (a) Lang, G.; Spartalian, K.; Reed, C. A.; Collman, L. *J. Chem. Phys.* **1978**, *69*, 5424. (b) Goff, H.; La Mar, G. N.; Reed, C. A. *J. Am. Chem. Soc.* **1977**, *99*, 3641.
(27) Estrin, D. A.; Corongiu, G.; Clementi, E. In *METECC, Methods and Techniques in Computational Chemistry*; Clementi, E., Ed.; Stef: Cagliari, Italy, 1993.
(28) Kohn, W.; Sham, L. J. *Phys. Rev.* **1965**, *A140*, 1133.
(29) Becke, A. D. *J. Chem. Phys.* **1988**, *88*, 1053.
(30) Godbout, N.; Salahub, D. R.; Andzelm, J.; Wimmer, E. *Can. J. Chem.* **1992**, *70*, 560.

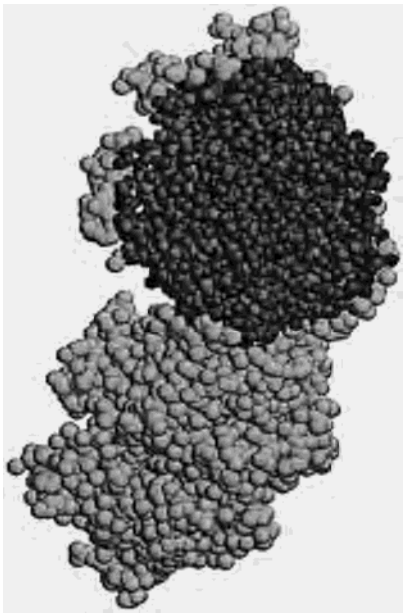

Figure 2. X-ray structure of cytochrome P450 Bm3. The enzyme has two chains, containing one heme each. Atoms excluded from the calculation (not enclosed in the cutoff) are displayed in soft gray. The structure was taken from ref 18.

(621,41,1) for C, N, and O. The auxiliary Coulomb basis sets used for expanding the electronic density were taken from ref 32 in the cases of C, N, and O (1111111/11/11), from ref 31 in the case of Fe (1111111111111/111/111), and from ref 30 for H (1111) and S (111111111/1111/1111). Computations were accomplished within the local density and the generalized gradient approximations (LDA and GGA). The Vosko−Wilk-Nusair correlation functional[33] was adopted for the LDA computations. In the case of GGA, we used the Becke and Perdew combination of functionals for exchange and correlation, respectively.[34]

The Hybrid Classical Mechanical−Quantum Mechanical Scheme. The protein environment effects on the active-site electronic structure were modeled by using a hybrid molecular mechanical-quantum mechanical scheme (MM-QM).[35] The QM subsystem corresponds to the active-site model described above. For the classical subsystem, we have taken into account 7091 atoms enclosed in a cutoff of 30 Å from the central iron. Figure 2 shows the X-ray structure of the cytochrome, exhibiting the atoms considered explicitly in the calculation. The total energy is given by the sum of the energy of the quantum mechanical subsystem E_{KS} and a coupling term E_{qm-cm}.

$$E_{KS}[\rho] = -\frac{1}{2}\sum_i \int \psi_i(\mathbf{r})\,\nabla^2\psi_i(\mathbf{r})\,d\mathbf{r} + \frac{1}{2}\int\int \frac{\rho(\mathbf{r})\,\rho(\mathbf{r}')}{|\mathbf{r}-\mathbf{r}'|}\,d\mathbf{r}\,d\mathbf{r}' + E_{xc}[\rho(\mathbf{r})] + \sum_\alpha \int \frac{\rho(\mathbf{r})\,z_\alpha\,d\mathbf{r}}{|\mathbf{r}-\tau_\alpha|} \quad (1)$$

$$E_{qm-cm} = \sum_i q_i \int \frac{\rho(\mathbf{r})}{|\mathbf{r}-\mathbf{R}_i|}\,d\mathbf{r} + \sum_{i,\alpha} \frac{q_i z_\alpha}{|\mathbf{R}_i-\tau_\alpha|} \quad (2)$$

In the first equation, $\psi_i(\mathbf{r})$ represents one-electron molecular orbitals and $E_{xc}[\rho(\mathbf{r})]$ the correlation and exchange contributions to the potential energy. τ_α and z_α are the coordinates and nuclear charges of the quantum subsystem, and $\mathbf{R}_i$ represents the coordinates of the atomic partial charges q_i of the protein. Both terms depend on the electronic density $\rho(\mathbf{r})$ of the quantum subsystem, obtained by solving self-consistently the Kohn−Sham equations[28] according to the procedure described above, including the protein electrostatic potential. The atomic point charges were assigned according to the AMBER molecular mechanics parametrization.[36] The usual classical mechanics contribution to the energy, which depends only on $\mathbf{R}_i$ and q_i, was not calculated because it remained constant in our computations.

Table 4. Relative Energies for the Different Spin States (kcal/mol)[a]

	R−FeP−H_2O			R−FeP−NO		
	doublet	quartet	sextet	singlet	triplet	quintet
gas phase, LDA	0	53.9	88.5	0	18.1	61.0
gas phase, GGA	0	41.6		0	12.6	52.8
protein, GGA	0	35.1		0	16.0	
gas phase, SAM1	0	12.8	49.1	0	27.0	29.2

[a] R−FeP represents the iron(III) porphyrin plus the cysteinyl residue.

Results and Discussion

With the aim of describing the substrate-free enzyme, the computations were performed on the iron(III) complexes. In this oxidation state, the system has no net charge and the total number of electrons is odd. Therefore, when the ligand is H_2O, the three lowest accessible spin states are a doublet, a quartet, and a sextet, which become a singlet, a triplet, and a quintet when the ligand is NO.

The Aquo Complex. The aquo complex is a model of the P450 active site in the basal state. Table 1 shows the X-ray structural parameters of the system used in the calculations, together with the corresponding values for three other six- and five-coordinated iron porphyrins with a cysteine ligand. It is interesting to note how the coordination number determines the displacement of the iron out of the plane defined by the nitrogen atoms of the porphyrin. The asymmetry in the coordination sphere pushes up the central ion, such distortion being reflected in the Fe−N distances. It is not always possible to unambiguously define the out-of-plane distance, because the nitrogen atoms of the ring are not necessarily on a plane. However, regardless of which plane is chosen, the displacement observed in this case for the P450 Bm3 is quite small (less than 0.1 Å), characteristic of low-spin iron porphyrins.[8] Calculations prove this empirical rule to be true. Table 4 displays the relative energies of the lowest accessible spin states, computed using the different quantum methods: for all approaches, the ground state turns out to be a doublet. It is important to point out that these are not the adiabatic but the vertical energetic differences, resulting from single-point energy calculations performed at the X-ray-known ground state structure. Therefore, we consider the ground state spin configuration as the one that yields the lowest energy for the experimental structure.

As can be seen, all calculations agree in the relative order of the spin states. Even in the case of SAM1, which yields the smallest energetic separations, these are large enough to ensure that the aquo complex will have a low-spin configuration in its ground state. The energetic separation between the doublet and the quartet is systematically larger for LDA than for GGA. A recent study on the hexaaquoferric ion has shown that DFT at

(31) Andzelm, J.; Radzio, E.; Salahub, D. R. *J. Comput. Chem.* **1985**, *6*, 520.
(32) (a) Sim, F.; Salahub, D. R.; Chin, S.; Dupuis, M. *J. Chem. Phys.* **1991**, *95*, 4317. (b) Sim, F.; St.-Amant, A.; Papai, I.; Salahub, D. R. *J. Am. Chem. Soc.* **1992**, *114*, 4391.
(33) Vosko, S. H.; Wilk, L.; Nusair, M. *Can. J. Phys.* **1980**, *58*, 1200.
(34) (a) Perdew, P. W. *Phys. Rev.* **1986**, *B33*, 8800; **1986**, *B34*, 7406 (erratum). (b) Becke, A. D. *Phys. Rev.* **1988**, *A38*, 3098.
(35) (a) Elola, M. D.; Laria, D.; Estrin, D. A. *J. Phys. Chem. A* **1999**, *103*, 5105. (b) Stanton, R. V.; Little, L. R.; Merz, K. M. *J. Phys. Chem.* **1995**, *99*, 17344.
(36) (a) Weiner, S. J.; Kollman, P. A.; Case, D. A.; Singh, U. C.; Ghio, C.; Alagona, G.; Profeta, S.; Weiner, P. *J. Am. Chem. Soc.* **1984**, *106*, 765. (b) Weiner, S. J.; Kollman, P. A.; Nguyen, D. T.; Case, D. A. *J. Comput. Chem.* **1986**, *7*, 230.

Table 5. Unpaired Spin Mulliken Populations for the Ground State of the Aquo Complex, Calculated Using DFT at the Generalized Gradient Approximation Level[a]

	Fe	S	O (H_2O)	C_2
gas phase	0.568	0.437	0.011	0.022
protein	0.635	0.363	0.017	0.018

[a] The atoms that are not shown in the table presented values below 0.01.

the GGA level provides reasonable values for spin state vertical transition energies, the magnitude of which, in the case of the iron complex, was overestimated by conventional ab initio techniques such as unrestricted Hartree−Fock or Møller−Plesset MP2 calculations.[13]

The unpaired spin Mulliken population offers very interesting information regarding the complex reactivity. Table 5 gives the unpaired spin populations on the Fe and the proximate atoms computed as $P^{\mathrm{spin}}(\mathrm{A}) = \sum_{\mu}[P^{\alpha}_{\mu\mu} - P^{\beta}_{\mu\mu}]S_{\mu\mu}$, where P is the density matrix, S is the overlap integral, and μ indicates basis functions centered on atom A. The LDA values, not shown, do not differ significantly from those yielded by GGA. The unpaired electron population is distributed mostly among two atoms: the iron and the sulfur. The adjacent oxygen does not significantly share this unpaired electron density, although the Fe−O length is slightly smaller than the Fe−S distance. This high localization of the unpaired electron will be important in the reactivity of the active site, particularly when interacting with a radical as NO. The spin population analysis indicates that the affinity of a radical for the sulfur atom linked to the metal should not be neglected. Actually, we expect a competition between the Fe and the S atoms as acceptors of the unpaired spin density of the nitric oxide. Previous computations[12a] performed using a mixture of DFT and unrestricted Hartree−Fock methods for the iron(III) *S*-methyl porphyrin aquo complex indicate that an appreciable amount of spin density (over 10%) is localized on the sulfur atom for the sextet. However, this is not observed in the doublet ground state, for which most of the unpaired electron density lies on the iron. The discrepancies between these and our results may proceed from the fact that different functionals and model systems were used.

A useful means to evaluate the reactivity of the system is the so-called Fukui function, $f(\mathbf{r})$, which is in fact the natural reactivity index of density functional theory.[37] This function is actually a derivative that will in general have one value from the right and one from the left. These two limits are denoted as $f^{+}(\mathbf{r})$ and $f^{-}(\mathbf{r})$, which in turn can be approximated by $\rho_{\mathrm{HOMO}}(\mathbf{r})$ and $\rho_{\mathrm{LUMO}}(\mathbf{r})$, respectively. The physical meaning of $f(\mathbf{r})$ is related to the chemical reactivity in the sense of the frontier electron theory.[38] In its context, the average of these indices is called $f^{0}(\mathbf{r})$ and measures reactivity toward a radical reagent.

$$f^{0}(\mathbf{r}) = {}^{1}/_{2}[f^{+}(\mathbf{r}) + f^{-}(\mathbf{r})] \approx {}^{1}/_{2}[\rho_{\mathrm{HOMO}}(\mathbf{r}) + \rho_{\mathrm{LUMO}}(\mathbf{r})] \quad (3)$$

Figure 3a depicts an isovalue contour of $f^{0}(\mathbf{r})$ according to the electronic density from the DFT calculation in vacuum at the GGA level. It can be seen that main contributions arise from the p and d orbitals of the sulfur and the iron. This evidence,

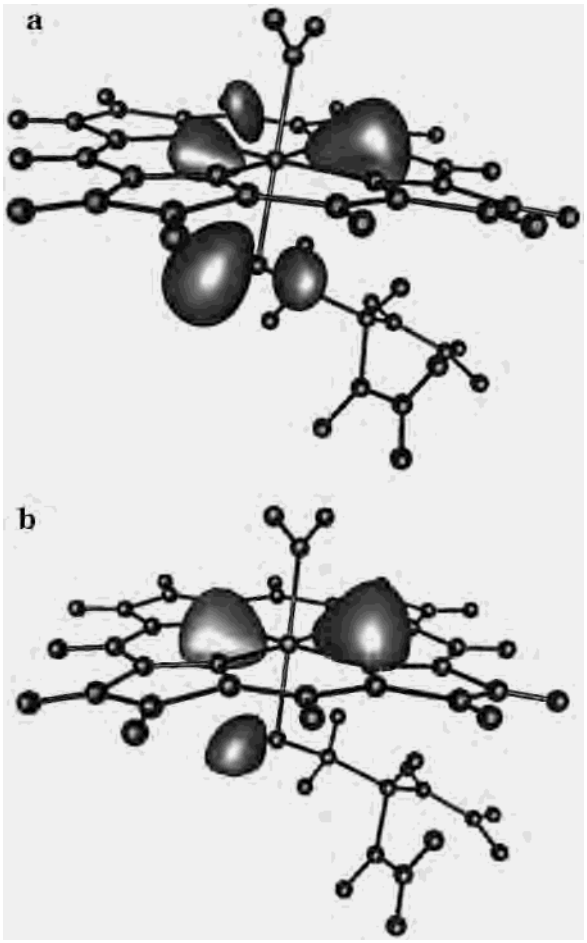

Figure 3. Fukui isovalue surfaces for the aquo complex: (a) in vacuum; (b) in the protein. The contours are plotted for $f^{0}(\mathbf{r}) = 0.075$ au.

added to the unpaired spin Mulliken population analysis, confirms that the attack of NO would be restricted to either of these two atoms. In fact, it is believed that NO has the ability to bind the sulfur atom of P450, and this reaction has also been proposed as a mechanism of inhibition. There is experimental evidence[7] showing that NO can interact with P450 in two ways: nitric oxide may reversibly bind to the heme moiety of P450, forming iron nitrosyl complexes, and may also irreversibly inactivate P450 via the nitrosylation of the proximate thiolate.

The Nitrosyl Complex. As mentioned above, there are no experimental geometries for the nitrosyl heme of cytochrome P450. It is shown by comparison of experimental data, and also by theoretical results (see, for example, refs 16 and 17), that, because of the rigidity of the ring, the internal coordinates of the porphyrin hardly change with the nature of the ligand or with the spin state. For this reason, the structure of the nitrosyl heme porphyrin was assumed to be the same as the structure of the aquo heme complex. A nitric oxide molecule was inserted in place of the water ligand, the coordinates of the nitric oxide being optimized using SAM1 calculations. The starting geometry was chosen to be close to that of the X-ray structure of nitrosyl hemoglobin.[39] In Table 4, we present the relative energies of the different spin states. The computations show that, also in this case, the ground state has a low-spin configuration. The

(37) Parr, R. G.; Yang, W. *Density-Functional Theory of Atoms and Molecules*; Oxford University Press: New York, 1990.

(38) (a) Fukui, K. *Theory of Orientation and Stereoselection*; Springer-Verlag: Berlin, 1975. (b) Fukui, K. *Science* **1987**, *218*, 747. (c) Fukui, K.; Yonezawa, T.; Shingu, H. *J. Chem. Phys.* **1952**, *20*, 722. (d) Fukui, K.; Yonezawa, T.; Nagata, C.; Shingu, H. *J. Chem. Phys.* **1954**, *22*, 1433.

(39) Vasquez, G. B.; Ji, X.; Pechik, I.; Fronticelli, C.; Gilliland, G. L. *X-ray Structure of Alpha-Oxy, Beta-(C112g)deoxy Human Hemoglobin.* PDB Code: 1GBV. Protein Data Bank at the National Library of Medicine. URL: http://www.ncbi.nlm.nih.gov.

Table 6. SAM1 Optimized Geometrical Parameters of the Nitrosylated Fe(III) Active Site (Distances, Å; Angles, deg)[a]

	singlet	triplet	quintet	experimental
Fe−N−O	178.7	151.1	143.3	175.6 (3.0)
Fe−N	1.70	1.80	1.92	1.66 (0.05)
N−O	1.17	1.17	1.18	1.11 (0.08)

[a] The experimental values are averages evaluated on seven model compounds,[41] with the standard deviations in brackets.

combination of two radical species produces a pairing of spin densities, leading to the formation of a singlet. These results, as well as those for the aquo complex, are in agreement with the current observed tendency for six-coordinated iron porphyrins to be low spin.[40] Again, the LDA energy gaps are larger than the ones computed with GGA.

Table 6 shows relevant geometrical parameters of the optimized nitrosyl complex for the three spin states considered. In the same table, we include experimental values measured for a series of hexacoordinate nitrosyliron(III) porphyrin derivatives. The reported parameters are mean values proceeding from the model compounds considered in ref 41,[41] with the corresponding standard deviations. These angles and bond lengths show a good correlation with those yielded by the semiempirical calculation of the ground state of the nitrosylated active site. No experimental estimations of geometries of higher energy spin states are available. However, with respect to these geometries, there is an interesting analysis that can be made in the context of the electron-counting formalism of Enemark and Feltham.[42] Within this formalism, useful to describe metalloporphyrin nitrosyls, the MNO group (M is the metal) is treated as an independent unit because it is considered to be the entity responsible for the ligation modes. In the notation $\{MNO\}^n$, n indicates the number of metal d electrons plus the electron in the π^* orbitals of NO. Hence, the ferric or iron(III) oxidation state is associated with the $\{FeNO\}^6$ scheme and the ferrous or iron(II) state with $\{FeNO\}^7$. In the $\{FeNO\}^6$ compounds, the Fe−N−O geometry is linear, and when the number of the d electrons increases, the geometry turns to bend: in $\{FeNO\}^7$, the angle is around 145°, while in $\{MNO\}^8$—as in Co(II) nitrosyls—it is ∼120°.[41] This structural change is understood in terms of a stabilization of the antibonding d_{z^2} and d_π orbitals caused by the bending of the M−N−O group. In the $\{FeNO\}^6$ complexes, these orbitals are empty, but in the $\{MNO\}^7$ and $\{MNO\}^8$ complexes, one of them becomes occupied. An alteration in the M−N−O angle and in the M−N distance allows a relaxation in the antibonding orbitals by weakening the d_{z^2}−n_{NO} and the d_{xz}−π^*_{NO} overlaps.[41,43] This behavior explains the trend observed in the higher energy spin states of the iron(III) nitrosyl (Table 6). For the singlet, examination of the orbitals shows that the HOMO has bonding character, while the next two orbitals—LUMO and $LUMO^{+1}$—have not. In the triplet and the quintet, one or both of the latter orbitals are populated, so it is expected for them to follow a structural trend similar to that observed in $\{MNO\}^7$ and $\{MNO\}^8$ species. In the case of the triplet, whose electronic structure resembles that of $\{MNO\}^7$ species, the Fe−N−O angle is very close to the angle measured in Fe(II) nitrosyls and the Fe−N distance is lengthened to the same extent (for $\{FeNO\}^7$ species, reported distances are between 1.72 and 1.80 Å; see ref 41). The difference between the electronic configurations of the quintet and the $\{MNO\}^8$ species is larger because, though both of them present the same number of antibonding electrons, the former has two half-occupied bonding orbitals. Nevertheless, the tendency to lengthen the Fe−N bond and to diminish the Fe−N−O angle is still apparent, although in the quintet the geometry relaxation effect seems to be more significant in the distance than in the angle (ref 41 reports experimental M−N distances between 1.83 and 1.86 Å).

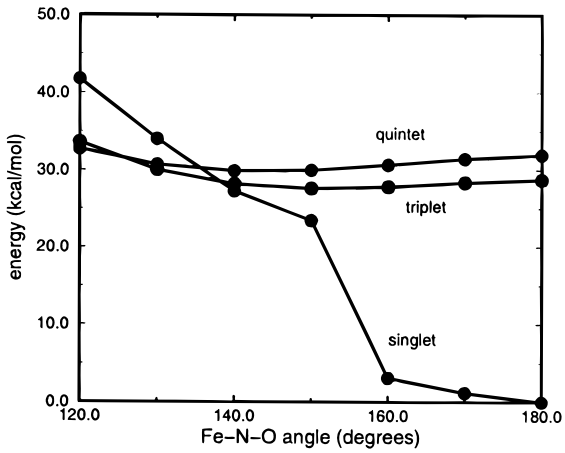

Figure 4. Potential energy surface for the bending of NO in the active site, corresponding to the three lowest accessible spin states.

The variation of the energy of each spin state versus the Fe−N−O angle (Figure 4) provides an estimation of the magnitude of the stabilization derived from the bending. The graph plotted in Figure 4 was obtained with SAM1 relaxing the N_α−Fe−N−O torsion and the Fe−N distance for each angle, with N_α, the porphyrin nitrogen, placed approximately over the carbon bound to the sulfur (N_α−Fe−S−C dihedral angle = 5.6°). It is seen that, similar to what is observed for other iron porphyrins with diatomic ligands, the total energy is not very much affected by changes in this dihedral angle, the torsion being almost free. The potential energy surfaces of the excited spin states are very shallow, which means that the stabilization due to bending is small (according to SAM1 results, it is not larger than 2 kcal/mol). However, it is enough to cause the significant perturbations observed in the geometries. On the other hand, Figure 4 shows that, for the singlet ground state, where no antibonding electrons are involved, the bending implies a higher energetic cost.

Ligand Exchange Energetics. Let us now focus on the reaction between the aquo complex and NO. The relevance of this process, as already remarked, lies in the fact that it might be the key to the inactivation of P450. The model process is the following:

$$\text{R−FeP−H}_2\text{O}\ (S = {}^1/_2) + \text{NO}\ (S = {}^1/_2) \rightarrow \text{R−FeP−NO}\ (S = 0) + \text{H}_2\text{O}$$

The notation R−FeP represents the iron porphyrin plus the cysteine residue. In Table 7 we present the DFT energetic changes calculated as $\Delta E_r = E(H_2O) + E(RFeP{\cdot}NO) - E(NO) - E(RFeP{\cdot}H_2O)$, where E refers to the total energies of the respective ground states. To obtain ΔE_r in the protein environment, the energies of H_2O and NO were computed using an

(40) (a) Collman, J. P.; Sorrell, T. N.; Hoffman, B. M. *J. Am. Chem. Soc.* **1975**, *97*, 913. (b) Collman, J. P.; Sorrell, T. N.; Hodgson, K. O.; Kulshrestha, A. K.; Strouse, C. E. *J. Am. Chem. Soc.* **1977**, *99*, 5180. (c) English, D. R.; Hendrickson, D. N.; Suslick, K. S.; Eigenbrot, C. W.; Scheidt, W. R. *J. Am. Chem. Soc.* **1984**, *106*, 7258.
(41) Scheidt, W. R.; Ellison, M. K. *Acc. Chem. Res.* **1999**, *32*, 350.
(42) Enemark, J. H.; Feltham, R. D. *Coord. Chem. Rev.* **1974**, *13*, 339.
(43) (a) Hoffmann, R.; Chen, M. M. L.; Elian, M.; Rossi, A. R.; Mingo, D. M. P. *Inorg. Chem.* **1974**, *13*, 2666. (b) Wayland, B. B.; Olson, L. W. *J. Am. Chem. Soc.* **1974**, *96*, 6037.

Onsager scheme with a dielectric constant equal to 78.5, to reproduce the conditions of aqueous solvation.[24,44] The results indicate that in the gas phase, as well as in the protein, the reaction is highly exergonic, so the substitution of H_2O by NO will be expected to prevail even under low concentrations of nitric oxide. Since the geometry of the active site was not allowed to relax, ΔE_r will correspond precisely to the difference of bond energies. This means that, in the complex, the Fe−N(NO) bond is much stronger than the Fe−O(H_2O) bond. In recent studies, the equilibrium constants of the reversible binding of NO to different ferrihemoproteins were obtained in aqueous solution.[45] The measured values, corresponding to ferricytochrome *c*, metmyoglobin, and methemoglobin, were in the range of 10^4 M^{-1}. On the assumption that, for this reaction, $\Delta G_r \approx \Delta E_r$, we find that the values of ΔE_r in solution should be around 5 kcal/mol, a quantity of the order of that predicted by our DFT computations. It must be taken into account that the coordination of iron is different in the hemoproteins investigated in the experiments, where the proximal ligand is histidine, as compared with the case of P450, where it is cysteine.

In vacuum as well as in the presence of the protein electrostatic potential, GGA yields less negative values for ΔE_r. This point is easily clarified if we consider that LDA bond energies are systematically larger than GGA energies (sometimes up to 100%)[46−49] and that NO binds more strongly to the active site than H_2O. This explains the trend in the values of ΔE_r, which differ by around 50%.

Effect of the Protein. The environment may affect a molecular system in an essential way, and it is known that, in many situations, the solvent enables a process that would not occur in the gas phase. In our case, where the active site is not exposed to the aqueous solution but placed deep inside the tertiary structure of P450, the environment is mainly hydrophobic, and therefore we do not expect properties to drastically differ from those manifested in vacuum.[20] However, ignoring the magnitude of this electrostatic field and how large its influence could be, it is of primary interest to establish to what extent the behavior of the active site is modulated by the presence of the protein. This analysis takes on importance not only for what concerns the particular case of P450 but also for assessing the capability of experimental results proceeding from isolated model systems to describe the active site under physiological conditions.

The first aspect we want to examine is the spin state. Table 4 shows that the energy gap between the low and the intermediate spin configurations becomes smaller when the ligand is water and larger when it is NO. However, in both cases, the protein electrostatic field provokes slight perturbations that are far from causing an inversion in the order of the spin states. Interestingly, the spin density appears to be more sensitive to the electrostatic field. In fact, the presence of the protein promotes a transference of spin density from the sulfur to the metal (Table 5). After incorporation of the electrostatic potential, the spin Mulliken population on the iron rises from 0.568 to 0.635, while on the sulfur it falls from 0.437 to 0.363, remaining practically constant on all other nuclei. These results suggest that experimental data corresponding to model porphyrins may be useful in predicting the ground spin state of the porphyrin in the enzyme, which seems to be a property controlled by the coordination mode, but the same would not necessarily hold for the prediction of other parameters: for example, values of *g* from EPR studies performed on isolated iron porphyrins might significantly differ from the values in the protein. On the other hand, the localization of the unpaired electron is expected to be to a greater extent responsible for the interaction between the NO and the active site. As already mentioned, the reaction of the nitric oxide with the sulfur atom of the proximal cysteine could be an alternative mechanism of P450 inactivation, via an irreversible thiol modification pathway.[7] The shifts in the spin populations upon the incorporation of the electrostatic potential suggest that the presence of the protein diminishes the reactivity of the sulfur. This conclusion is reinforced by the examination of the mean value of the Fukui function for the system with and without the electrostatic field (Figure 3). We can clearly appreciate the effect of the protein on the distribution of the electronic densities of the HOMO and the LUMO, reflected in the $f^0(\mathbf{r})$ isosurfaces: some density disappears from the sulfur and concentrates around the iron. In this way, the trends manifested in the spin population are consistent with the changes observed in $f^0(\mathbf{r})$. Although it is questionable whether the inhibition of cytochrome P450 proceeds through the formation of an iron nitrosyl adduct or through thiol nitrosylation, the fact is that both pathways are likely to occur. At this point, what we can say is that, if such competition exists, the protein will favor the reaction ratio toward the iron atom.

Table 7. Reaction Energies for the Ligand Exchange (kcal/mol)

gas phase, LDA	gas phase, GGA	protein, LDA	protein, GGA
−28.1	−18.0	−24.6	−14.5

Finally, looking at the overall thermodynamics of the ligand exchange (Table 7), we find that the protein reduces ΔE_r for 12% in LDA and by 20% in GGA. It is clear that the electrostatic potential opposes the reaction, but not so much as to prevent it from happening. Thereby, this decrease places the value of ΔE_r even closer to the values reported for other hemoproteins in ref 46. The presence of the protein, of course, involves other aspects to consider, such as, for example, the accessibility of NO to the cavity beside the active site. This concerns the dynamics of the whole process, which is beyond the scope of this work.

Conclusions

The present work has assessed the feasibility of the displacement of H_2O by NO as the first step in the reversible inhibition of cytochrome P450. To study the reaction, the electronic configuration of the involved species was examined: in both complexes the ground states turned out to be low spin. The electronic densities corresponding to the HOMO and the LUMO of the aquo complex have also been investigated, exhibiting a preferential distribution around the iron and the sulfur atoms. This result, together with the high localization of the spin population, establishes that the attack of nitric oxide on the active site will occur at either of these sites. The possibility of an interaction between NO and the sulfur of the cysteine as an alternative mechanism of enzyme inhibition probably involves

(44) Wong, M. W.; Wiberg, K. B.; Frisch, M. J. *J. Am. Chem. Soc.* **1992**, *114*, 1645.
(45) Hoshino, M.; Maeda, M.; Konishi, R.; Seki, H.; Ford, P. *J. Am. Chem. Soc.* **1996**, *118*, 5702.
(46) Ziegler, T. *Chem. Rev.* **1991**, *91*, 651.
(47) (a) Li, H.; Poulos, T. L. *Acta Crystallogr.* **1995**, *D51*, 21. (b) Schlichting, I.; Jung, C.; Schulze, H. *FEBS Lett.* **1997**, *3*, 253. (c) Sundaramoorthy, M.; Terner, J.; Poulos, T. L. *Structure* (*London*) **1995**, *3*, 1367.
(48) (a) Peng, S. M.; Ibers, J. A. *J. Am. Chem. Soc.* **1976**, *98*, 8032. (b) Scheidt, W. R.; Frisse, M. E. *J. Am. Chem. Soc.* **1975**, *97*, 17. (c) Jameson, G. B.; Rodley, G. A.; Robinson, W. T.; Gagne, R. R.; Reed, C. A.; Collman, J. P. *Inorg. Chem.* **1978**, *17*, 850.
(49) Momenteau, M.; Reed, C. A. *Chem. Rev.* **1994**, *94*, 659.

the breaking of the Fe−S bond, leading to structural changes in the protein backbone. For this reason, the modeling of this reaction pathway has been left for further studies. Moreover, we saw that the electrostatic field of the protein does not affect the ground spin state or the thermodynamic viability of the reaction but that it does significantly modify the magnitude of the energetic changes and the localization of the unpaired electron in the resting state of P450.

Acknowledgment. This work was partially supported by the Fundación Antorchas and the University of Buenos Aires. D.A.E. is a member of the scientific staff of CONICET (National Scientific Council, Argentina). D.A.S. acknowledges CONICET for a doctoral fellowship. We are also grateful to J. Pedemonti for useful discussions.

IC991191D